Isocyanide Insertion Chemistry. Synthesis and Structural Characterization of Bridging Imidoyl Complexes of Nickel and Amide Formation by Intramolecular Coupling of Acyl and Imidoyl Functionalities

Juan Câmpora,[1a] Enrique Gutiérrez,[*,1b] Angeles Monge,[1b] Manuel L. Poveda,[*,1a]
Caridad Ruiz,[1b] and Ernesto Carmona[*,1a]

Departamento de Química Inorgânica-Instituto de Ciencia de Materiales, Universidad de Sevilla-CSIC, Apdo 553, 41071 Sevilla, Spain, Instituto de Ciencia de Materiales, Sede D, CSIC, Serrano, 113, 28006 Madrid, Spain, and Facultad de Ciencias Químicas, Universidad Complutense, 28040 Madrid, Spain

Received March 29, 1993[⊗]

The binuclear pseudoallyl complex *trans*-$(Me_3P)BrNi(\mu_2\text{-}\eta^3{:}\eta^1\text{-}CH_2\text{-}o\text{-}C_6H_4)NiBr(PMe_3)_2$ (1) inserts selectively 1 equiv of CNXy (Xy = 2,6-dimethylphenyl) into the Ni—benzylic bond with formation of the cyclic complex *trans*-$(Me_3P)_2BrNi(C(NXy)CH_2\text{-}o\text{-}C_6H_4)NiBr(PMe_3)$ (2) that contains a bridging η^2-imidoyl ligand. The analogous reaction of 1 with CNBu^t gives a related μ_2,η^2-imidoyl species **3a** which, in contrast to **2**, exists in solution in thermodynamic equilibrium with its isomer *trans*-$(Me_3P)BrNi(\eta^2\text{-}C(NBu^t)CH_2\text{-}o\text{-}C_6H_4)NiBr(PMe_3)_2$ (**3b**), in which the imidoyl ligand is terminally bonded in a η^2 fashion to one of the nickel centers. Variable temperature NMR studies show **3b** is the kinetic product of the insertion reaction and that the strongly solvent dependent equilibrium **3a** ⇌ **3b** is attained only at sufficiently high temperatures (ca. −20 °C). At even higher temperatures (ca. 40 °C), the **3a**–**3b** mixtures convert into a third isomeric compound, *trans*-$(Me_3P)_2Ni(C(NBu^t)C_6H_4\text{-}o\text{-}CH_2)NiBr(PMe_3)$ (4), in a process which formally corresponds to the deinsertion of CNBu^t from the Ni—benzyl bond followed by reinsertion into the Ni—aryl moiety. In a rather complex reaction **2** interacts with CO to afford the mononuclear complex *trans*-$Ni(C{=}CHC_6H_4C(O)NXy)Br(PMe_3)_2$ (5) whose formation probably involves the intramolecular coupling of acyl and imidoyl functionalities. Hydrolytic cleavage of the Ni—C bond in **5** provides the corresponding *N*-aryl-1-isoquinolone **6**. Compounds **2** and **3a**, have been characterized by X-ray studies. **2** crystallizes in the monoclinic space group $P2_1/n$ with a = 12.437(3) Å, b = 16.025(2) Å, c = 16.015(2) Å, β = 101.47(1)°, and Z = 4. Crystals of **3a** are also monoclinic, space group $P2_1/n$, with a = 26.05(1) Å, b = 10.226(1) Å, c = 12.013(2) Å, β = 93.54(12)°, and Z = 4. The μ_2,η^2-imidoyl functionalities of both complexes exhibit similar structural characteristics.

The chemistry of transition metal binuclear complexes in which the two metal centers are maintained in close proximity by bridging hydrocarbon ligands has aroused considerable interest in recent years because of the unusual reactivity patterns that sometimes appear due to the cooperative effects between the two metal units.[2] As part of our ongoing studies on the insertion reactions of CO and CNR into transition metal–carbon bonds, we have recently explored the reactivity toward CO of one such system, the pseudoallyl complex *trans*-$(Me_3P)BrNi(\mu_2\text{-}\eta^3{:}\eta^1\text{-}CH_2\text{-}o\text{-}C_6H_4)NiBr(PMe_3)_2$ (1), and found,[3] among other features, that it inserts selectively 1 equiv of CO into the Ni–aryl bond (eq 1). Isocyanide ligands are in many aspects similar to CO and often exhibit analogous features with respect to insertion reactions.[4] Some important differences between CO and CNR insertions have, however, been noted, among them (i) the greater tendency of imidoyl ligands (as compared with acyls) to bond in a η^2 fashion together with the possibility of having more than one η^2-imidoyl ligand bound to the same metal center;[4a] (ii) the propensity of isocyanides to undergo polyinsertions;[5] and (iii) the stability of imidoyls toward deinsertion, in contrast to the well-known reversibility of the CO insertion reaction.

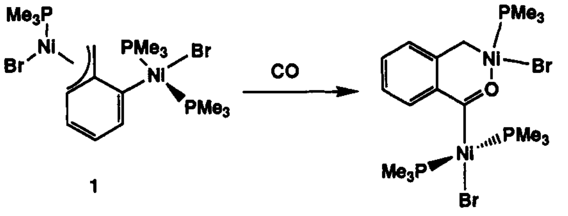

(1)

As an extension of the above studies we have now investigated the reactivity of 1 toward two isocyanides, CNXy (Xy = 2,6-dimethylphenyl) and CNBu^t, and report herein the results of this study. In the latter case (CNBu^t) and probably due to the steric bulkiness of the CNBu^t

---

[⊗] Abstract published in *Advance ACS Abstracts,* August 15, 1993.

(1) (a) Universidad de Sevilla-CSIC. (b) CSIC and Universidad Complutense.

(2) (a) Holton, J.; Lappert, M. F.; Pearce, R.; Yarrow, P. J. W. *Chem. Rev.* **1983**, *83*, 135. (b) Moss, J. R.; Scott, L. G. *Coord. Chem. Rev.* **1984**, *60*, 171. (c) Casey, C. P.; Andett, J. D. *Chem. Rev.* **1986**, *86*, 339.

(3) Câmpora, J.; Gutiérrez, E.; Monge, A.; Poveda, M. L.; Carmona, E. *Organometallics* **1992**, *11*, 2644.

(4) (a) Durfee, L. D.; Rothwell, I. P. *Chem. Rev.* **1988**, *88*, 1059. (b) Alexander, J. J. In *The Chemistry of the Metal-Carbon Bond*; Hartley, F. R., Patai, S., Eds.; Wiley: New York, 1985; Vol. 2, Chapter 5.

0276-7333/93/2312-4025$04.00/0

ligand, we have found a remarkable variety of insertion products (**3a**,**b** and **4**). We have also achieved successive insertion of CNXy and CO into the Ni–C bonds of **1** followed by intramolecular coupling of the resulting imidoyl and acyl functionalities and formation of a vinyl complex of nickel derived from *N*-aryl-1-isoquinolone. A preliminary account of this is available.[6]

Results and Discussion

Reaction of 1 with CNXy. Tetrahydrofuran solutions of the pseudoallylic complex **1** smoothly react with 2,6-dimethylphenyl isocyanide, CNXy, to afford a crystalline species **2** in 65% isolated yield. Monitoring of the reaction by low temperature $^{31}P\{^1H\}$ NMR spectroscopy shows that the consumption of **1** starts as low as −60 °C and that formation of **2** occurs cleanly without detectable intermediates. The new compound has been characterized by analytical data (including molecular weight measurements) and spectroscopic studies as the μ_2,η^2-imidoyl species shown in eq 2. Hence, CNXy inserts selectively into the Ni–CH$_2$ bond of **1**, the resulting imidoyl functionality also bonding the second nickel center by means of the N lone pair. The precise site of insertion (namely the Ni–benzylic or the Ni–C aromatic bonds) of the molecule of CNXy can be determined unambiguously by spectroscopy. Thus, the $^{13}C\{^1H\}$ resonance due to the Ni–CH$_2$ group shifts considerably to low field and appears in **2** at δ 58.9, while the intact Ni–C$_{aryl}$ unit gives rise to a doublet at δ 152.6 ($^2J_{CP}$ = 44 Hz). This coupling constant, although relatively large, is still below the 50–80-Hz range associated with *trans* couplings in compounds of this type.[7]

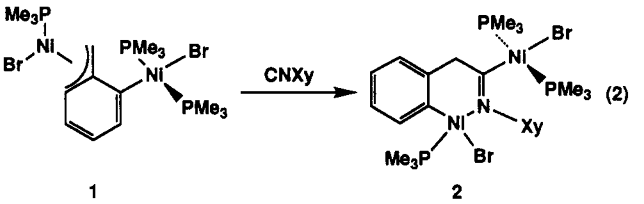

On the other hand, the imidoyl functionality gives rise to an IR absorption at 1495 cm^{-1} and to a $^{13}C\{^1H\}$ resonance due to the Ni-bound imidoyl carbon at δ 224. Although it seems that the value of ν(C=N) and the chemical shift of the M—C(NR′)R carbon cannot be used as consistent parameters for the assignment of the bonding mode of the imidoyl ligand,[4a,5f,8] a comparison of their values in a series of closely related compounds clearly allows us to distinguish between the possible bonding types. In 16-electron square-planar complexes of nickel containing PMe$_3$ as coligand,[8,9] a structure of type **A** (η^1-imidoyl) gives ν(C=N) at ca. 1600 cm^{-1}, while in formulation **B** this band is shifted to a higher frequency by about 100 cm^{-1}. $^{13}C\{^1H\}$ NMR data are less conclusive in this respect, although in complexes of this type δ(C=N) is consistently at a lower field in **A** than in **B**. As can be seen, ν(C=N) and δ(C=N) for **2** are not in the range expected for structures of types **A** or **B** and this, together with the binuclear nature of compound **2**, suggests a bridging η^2-imidoyl structure of the type depicted in **C** (this has been demonstrated by X-ray studies to be discussed below). This solid state structure is also maintained in solution, as indicated by the very similar values of ν(C=N) observed in the IR spectra of solid and dissolved samples of **2**. Bridging imidoyl complexes are not numerous, but the reported[10] ν(C=N) values are very close[11] to that found for **2**. Thus, despite the fact that there seems to be no direct involvement of the π C=N component in the bonding to the metal center,[10d] it appears that the implication of the N lone pair in a Lewis type donation with another metal fragment produces a decrease in the C—N bond order. Finally, with respect to the spectral characterization of **2**, the presence of the bulky xylyl substituent clearly hinders the rotation around the C—NiBr(PMe$_3$)$_2$ bond and makes inequivalent the *trans* phosphine ligands ($^{31}P\{^1H\}$ NMR: AB quartet with a large $^2J_{PP}$ of 267 Hz).

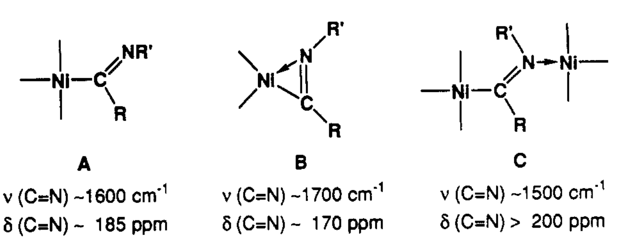

Figure 1 illustrates an ORTEP perspective view of the molecules of **2**, including the atom numbering scheme. Table I collects important bond distances and angles. The coordination sphere around the two nickel centers is distorted square-planar, with the two coordinated C atoms of the bridging hydrocarbon ligand occupying *trans* positions with respect to the corresponding bromides. The orientation of the bridging chain is such that in addition to optimizing the N→Ni(2) dative interaction, it allows the Ni-bonded aryl and C—imidoyl ligands to arrange themselves in positions nearly perpendicular to their respective coordination planes, that is, close to their preferred orientations.[12,13] Both the N and the C(1) atoms exhibit planar environments (the sum of the coordination angles is ca. 359° for both atoms), with the largest deviation from the ideal 120° angle corresponding to Ni(1)—C(1)—N (125.4(7)°). The Ni(1)—N and Ni(2)—C(1) distances of 2.835(8) and 2.827(9) Å, respectively, indicate the absence of bonding interactions between these pairs of atoms.

---

[5] (a) Otsuka, S.; Nakamura, A.; Yoshida, T.; Naruto, M.; Ataka, K. *J. Am. Chem. Soc.* **1973**, *95*, 3180. (b) Yamamoto, Y.; Yamazaki, H. *Inorg. Chem.* **1974**, *13*, 438. (c) Bellachiona, G.; Cardaci, G.; Zanazzi, P. *Inorg. Chem.* **1987**, *26*, 84. (d) Bochmann, M.; Hawkins, I.; Sloan, M. P. *J. Organomet. Chem.* **1987**, *332*, 371. (e) Carmona, E.; Marín, J. M.; Palma, P.; Poveda, M. L. *J. Organomet. Chem.* **1989**, *377*, 157. (f) Fandos, R.; Meetsma, A.; Teuben, J. H. *Organometallics* **1991**, *10*, 2665.

[6] Cámpora, J.; Carmona, E.; Gutiérrez, E.; Palma, P.; Poveda, M. L.; Ruíz, C. *Organometallics* **1992**, *11*, 11.

[7] (a) Neidlein, R.; Rufinska, A.; Schwager, H.; Wilke, G. *Angew. Chem., Int. Ed. Engl.* **1986**, *25*, 640. (b) Carmona, E.; Paneque, M.; Poveda, M. L. *Polyhedron* **1989**, *8*, 285. (c) Carmona, E.; Paneque, M.; Poveda, M. L.; Gutiérrez-Puebla, E.; Monge, A. *Polyhedron* **1989**, *8*, 1069.

[8] Carmona, E.; Palma, P.; Paneque, M.; Poveda, M. L. *Organometallics* **1990**, *9*, 583.

[9] Belderraín, T. R.; Gutiérrez, E.; Monge, A.; Paneque, M.; Poveda, M. L.; Sernau, V.; Carmona, E. Submitted for publication.

[10] (a) Usón, R.; Forniés, J.; Espinet, P.; Lalinde, E.; García, A.; Jones, P. G.; Meyer-Bäse, K.; Sheldrick, G. M. *J. Chem. Soc., Dalton Trans.* **1986**, 259. (b) Seyferth, D.; Hoke, J. B. *Organometallics* **1988**, *7*, 254. (c) Bertani, R.; Berton, A.; Di Bianca, F.; Crociani, B. *J. Organomet. Chem.* **1988**, *348*, 411. (d) Day, M.; Espitia, D.; Hardcastle, K. I.; Kabir, S. E.; Rosenberg, E. *Organometallics* **1991**, *10*, 3550.

[11] Only in polyfluorinated derivatives (R = C$_6$F$_5$) have larger ν(C=N) values (ca. 1600 cm^{-1}) been observed.[10a]

[12] (a) Churchill, M. R.; O'Brien, T. A. *J. Chem. Soc. A* **1969**, 266. (b) Klabunde, U.; Tulip, T. H.; Roe, D. C.; Ittel, S. D. *J. Organomet. Chem.* **1987**, *334*, 141. (c) Cámpora, J.; Gutiérrez, E.; Poveda, M. L.; Ruíz, C.; Carmona, E. *J. Chem. Soc., Dalton Trans.* **1992**, 1769.

[13] For related Ni–acyl structures, see: (a) Klein, H. F.; Karsch, H. H. *Chem. Ber.* **1976**, *109*, 2524. (b) Carmona, E.; González, F.; Poveda, M. L.; Atwood, J. L.; Rogers, R. D. *J. Chem. Soc., Dalton Trans.* **1980**, 2108.

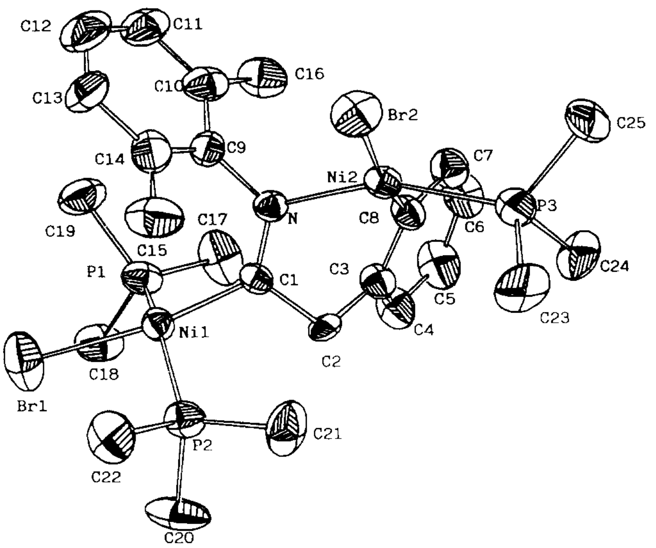

Figure 1. Molecular structure of compound **2**.

Table I. Bond Distances (Å) and Angles (deg) for 2

Ni1–Br1	2.380(2)	N–C9	1.453(12)
Ni1–P1	2.188(3)	C1–C2	1.528(13)
Ni1–P2	2.244(3)	C2–C3	1.506(14)
Ni1–C1	1.866(9)	C3–C4	1.384(15)
Ni2–Br2	2.381(2)	C3–C8	1.386(14)
Ni2–P3	2.164(3)	C4–C5	1.385(18)
Ni2–N	1.977(8)	C5–C6	1.381(18)
Ni2–C8	1.872(9)	C6–C7	1.406(15)
P1–C17	1.786(13)	C7–C8	1.387(15)
P1–C18	1.819(12)	C9–C10	1.426(15)
P1–C19	1.814(13)	C9–C14	1.379(17)
P2–C20	1.820(12)	C10–C11	1.381(15)
P2–C21	1.818(11)	C10–C16	1.488(17)
P2–C22	1.809(12)	C11–C12	1.387(23)
P3–C23	1.810(13)	C12–C13	1.351(21)
P3–C24	1.803(14)	C13–C14	1.396(16)
P3–C25	1.824(12)	C14–C15	1.493(16)
N–C1	1.312(11)		

P2–Ni1–C1	94.5(3)	Br2–Ni2–N	95.5(2)
P1–Ni1–C1	90.9(3)	Br2–Ni2–P3	91.7(1)
P1–Ni1–P2	158.1(1)	Ni2–N–C9	121.1(6)
Br1–Ni1–C1	169.1(3)	Ni2–N–C1	117.1(6)
Br1–Ni1–P2	88.4(1)	C1–N–C9	121.4(8)
Br1–Ni1–P1	90.3(1)	Ni1–C1–N	125.4(7)
N–Ni2–C8	88.6(4)	N–C1–C2	116.2(8)
P3–Ni2–C8	88.0(3)	Ni1–C1–C2	118.4(6)
P3–Ni2–N	156.9(2)	C1–C2–C3	113.0(7)
Br2–Ni2–C8	170.1(3)		

Therefore, structures of the types Ni(1)—C(1)=N—Ni-(2) and Ni(1)—C(1)=N—Ni(2) can be discarded.

The Ni(1)—C(1) bond length of 1.866(8) Å, although somewhat longer than the corresponding distance in the recently reported Ni(η^2-C(NBu^t)CH(SiMe$_3$)$_2$)Cl(PMe$_3$) complex,[9] is well in the 1.78–1.87-Å range normally found for complexes of this type.[13] The Ni(2)←N dative bond also has a normal length (1.977(8) Å) but is definitely longer than the analogous distance in the CH(SiMe$_3$)$_2$ derivative (1.82(1) Å). Finally, the C(1)—N separation of 1.312(11) Å is also longer than in η^1- and η^2-imidoyls[4a,5f,9,14] but compares well with organic C=N bonds[15] (1.26–1.31 Å). This relative enlargement could be caused partially by the geometrical requirements of the six-membered ring, that result in a torsion angle around the C=N bond of 18.2(4)° and, hence, in a slight deviation from the optimum overlap for π interaction.

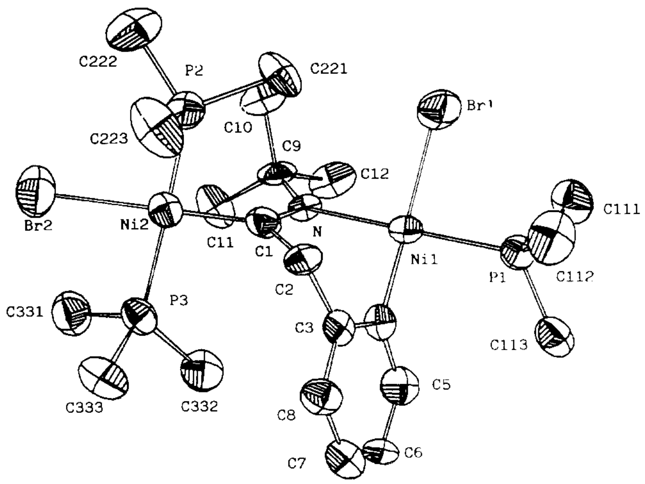

Figure 2. ORTEP view and atom labeling scheme of compound **3a**.

From the analysis of the bond distances and angles collected in Table I it can be concluded that the bonding within the metal—imidoyl linkage in **2** can be satisfactorily described by the simple model **D** with little or no

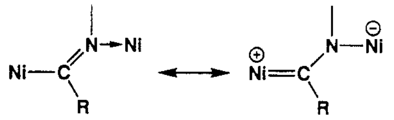

D **E**

contribution from other resonance forms, including the carbenoid structure **E**. It also seems clear that the Ni←N interaction is responsible for the decrease of the C—N bond order and of the value of ν(C=N). Nevertheless, in view of the complexity of the situation, care should be exercised when attempting to correlate these parameters.

1-CNBu^t System. (a) Reaction of 1 with CNBu^t. In a closely related process, complex **1** reacts with CNBu^t to afford an orange crystalline solid, **3a**, in 65% isolated yield. Analytical and spectroscopic data (ν(C=N) 1530 cm^{-1}, Nujol mull) for this crystalline solid suggest a μ_2-η^2-imidoyl structure similar to that of **2**. However, at variance with this compound, interesting behavior is found for the solutions of **3a** in common organic solvents. The room temperature ^{31}P{^{1}H} NMR spectrum of **3a** in acetone or dichloromethane is dominated by two singlets of intensity 2:1 (the second being somewhat broad). These are in discord with the structure assigned to **3a** and can therefore be attributed to a second species **3b**. In addition, there is a less intense pattern of resonances, very similar to that found for **2** (i.e. a singlet and a strongly coupled AB quartet, $^2J_{PP}$ = 235 Hz), in agreement with the formulation proposed for **3a**. The ratio of these two species, **3b**:**3a** in the above solvents is ca. 6.5 but changes to a value of about 1 upon removal of the solvent and redissolution of the residue in THF. This solvent dependence of the **3b**:**3a** ratio is fully reversible. Accordingly, the second isomeric species **3b** is in equilibrium with the μ_2-η^2-imidoyl complex **3a** and their interconversion is fast in the laboratory time-scale at room temperature. Crystallization of **3a**–**3b** mixtures (see Experimental Section) provides exclusively **3a**, which has been characterized by X-ray studies. Figure 2 shows an ORTEP perspective view of

---

[14] Adams, R. D.; Chodosh, D. F. *Inorg. Chem.* **1978**, *17*, 41.

[15] Sandorfy, C. In *The Chemistry of the Carbon-Nitrogen Double Bond*; Patai, S., Ed.; Wiley: New York, 1970; Chapter 1.

Table II. Bond Distances (Å) and Angles (deg) for 3a with Standard Deviations Given in Parentheses

Ni1–Br1	2.401(3)	P3–C332	1.82(2)
Ni1–P1	2.163(6)	P3–C333	1.80(2)
Ni1–N	1.96(1)	N–C1	1.28(2)
Ni1–C4	1.90(2)	N–C9	1.54(2)
Ni2–Br2	2.365(3)	C1–C2	1.52(2)
Ni2–P2	2.220(6)	C2–C3	1.50(2)
Ni2–P3	2.240(6)	C3–C4	1.37(2)
Ni2–C1	1.851(2)	C3–C8	1.41(3)
P1–C111	1.80(2)	C4–C5	1.43(3)
P1–C112	1.81(2)	C5–C6	1.40(3)
P1–C113	1.81(2)	C6–C7	1.34(3)
P2–C221	1.80(2)	C7–C8	1.37(3)
P2–C222	1.79(2)	C9–C10	1.52(3)
P2–C223	1.80(2)	C9–C11	1.50(3)
P3–C331	1.80(2)	C9–C12	1.55(3)

P1–Ni1–C4	91.8(5)	Ni2–P3–C331	114.3(8)
P1–Ni1–N	176.1(4)	C332–P3–C333	101.6(10)
Br1–Ni1–C4	161.1(5)	C331–P3–C333	104.0(10)
Br1–Ni1–N	93.1(4)	C331–P3–C332	99.9(10)
Br1–Ni1–P1	86.0(2)	C1–N–C9	121.9(13)
P3–Ni2–C1	93.4(6)	Ni2–C1–N	134.3(13)
P2–Ni2–C1	90.5(6)	N–C1–C2	113.3(15)
P2–Ni2–P3	166.2(2)	Ni2–C1–C2	112.3(12)
Br2–Ni2–C1	178.2(6)	C1–C2–C3	111.1(15)
Br2–Ni2–P3	88.0(2)	C2–C3–C8	119.8(16)
Br2–Ni2–P2	87.9(2)	C2–C3–C4	118.1(15)
Ni1–P1–C113	124.0(7)	C4–C3–C8	121.6(16)
Ni1–P1–C112	109.1(7)	Ni1–C4–C3	110.7(13)
Ni1–P1–C111	116.6(7)	Ni1–C4–C5	132.2(13)
C112–P1–C113	100.2(10)	C3–C4–C5	116.7(16)
C111–P1–C113	100.3(10)	C4–C5–C6	119.7(17)
C111–P1–C112	104.0(10)	C5–C6–C7	121.9(16)
Ni2–P2–C223	108.1(8)	C6–C7–C8	119.2(18)
Ni2–P2–C222	115.7(8)	C3–C8–C7	120.5(18)
Ni2–P2–C221	121.5(6)	N–C9–C12	106.9(14)
C222–P2–C223	105.7(10)	N–C9–C11	111.8(14)
C221–P2–C223	101.2(9)	N–C9–C10	109.7(14)
C221–P2–C222	102.8(10)	C11–C9–C12	108.4(15)
Ni2–P3–C333	110.0(7)	C10–C9–C12	109.2(15)
Ni2–P3–C332	124.6(7)	C10–C9–C11	110.8(15)

the molecules of this complex, and Table II summarizes important bond distances and angles. The bonding parameters for **3a**, in particular those concerning the bridging aryl—imidoyl ligand, are very similar to those already discussed for **2**, and for that reason, they will not be examined any further, except to briefly mention that in this case there seems to be no geometrical restrictions to C=N π bonding (torsion angle 178(1)°) and this could explain the increase in the value of ν(C=N) to 1530 cm^{-1}.

Dissolution of **3a** in CD$_2$Cl$_2$ at −40 °C yields almost spectroscopically pure solutions of this complex that display spectroscopic properties very similar to those of **2** (see Experimental Section), in accord with the proposed structure (Scheme I). At temperatures above −20 °C, **3a** converts into **3b** and the equilibrium **3a** $\rightleftharpoons$ **3b** is then restored.

Spectroscopic data for **3b** are in favor of the terminal η^2-imidoyl formulation shown in Scheme I. Thus, CD$_2$Cl$_2$ solutions of **3**, in which, as already indicated, **3b** is the main species present, display ν(C=N) at 1730 cm^{-1}, i.e. the frequency expected for a terminal η^2-imidoyl complex of nickel.[8,9] The observation of two singlets (2:1 ratio) in the ^{31}P{^{1}H} NMR spectrum is also in line with these arguments, since the PMe$_3$ ligands of the Ni—aryl moiety are expected to be equivalent. The ^{13}C{^{1}H} NMR spectrum provides more conclusive evidence in favor of this structure. The nickel-bound aromatic carbon appears as a triplet due to coupling to the two equivalent ^{31}P nuclei (δ 158, ${}^2J_{CP}$ = 34 Hz), while the imidoyl carbon yields a somewhat broad resonance at δ 169, that is in the region normally found for Ni—η^2-imidoyl functionalities, but with the expected carbon—phosphorus coupling being absent at room temperature. This last observation could be explained on the basis of a fast intermolecular exchange with traces of trimethylphosphine, with concomitant $\eta^2 \rightleftharpoons \eta^1$ change of the imidoyl ligand (hence the already mentioned observation of a slightly broad singlet for the corresponding ^{31}P{^{1}H} signal). Monitoring the conversion of **1** into **3** by means of low temperature ^{31}P{^{1}H} NMR spectroscopy using THF as the reaction solvent discloses that the disappearance of **1** starts at −50 °C, with only the terminal η^2-imidoyl **3b** being produced at this stage. Upon warming to −20 °C, formation of **3a** begins at the expense of **3b**, and as indicated above, at room temperature the thermodynamic **3a**:**3b** ratio is quickly established. Consequently, the primary kinetic product of the insertion is the terminal η^2-imidoyl which later transforms into the isomeric bridging imidoyl. A similar reaction pathway could be proposed for the formation of **2**, although in this system there seems to be a larger energy difference between the two isomers (in favor of the cyclic one, which is in fact the only one observed). The more sterically demanding CNBu^t group could make the cyclic imidoyl **3a** somewhat less thermodynamically and kinetically favorable with respect to the terminal isomer (as compared with the analogous species in the 1-CNXy system), thus allowing the observation of complex **3b**. Prior to the insertion reaction it seems reasonable that an intermediate η^1-benzyl complex may form, as a result of the addition of a molecule of isocyanide to the pseudoallylic complex **1**.

Scheme I

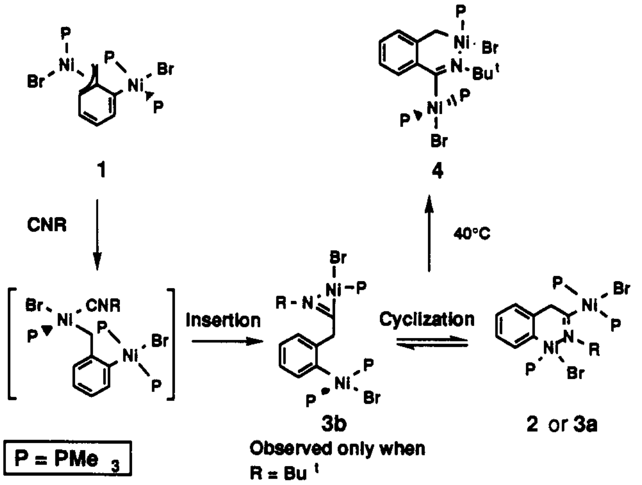

(b) Thermal Rearrangement of 3. Observation of a Formal 1,3-Isocyanide Shift. The thermal activation of an equilibrated mixture **3a** $\rightleftharpoons$ **3b** (acetone, 40 °C, 4 h) induces the formation of a third isomeric species, **4**, which is obtained as dark red crystals in ca. 55% isolated yield, together with an insoluble, untractable precipitate. Analytical and spectroscopic data for **4** are in accord with its formulation as a cyclic, μ_2,η^2-imidoyl derivative *but with the molecule of CNBu^t inserted into the Ni—C$_{aryl}$ bond* (Scheme I). Similarly to **2** and **3a**, complex **4** exhibits a low ν(C=N) frequency of ca. 1500 cm^{-1} and a low field ^{13}C{^{1}H} resonance (δ(C=N) 204 ppm, t, ${}^2J_{CP}$ = 27 Hz), but in contrast with these two compounds, the methylene carbon resonates at a relatively high field (δ 18) and arises as a doublet, with ${}^2J_{CP}$ = 25 Hz. This conclusively proves that the methylene group is bonded to one of the nickel centers[16] in a *cis* position[7] with respect to the unique phosphine ligand. As none of the aromatic quaternary carbons experience coupling to the phosphorus nuclei, it can be concluded that the Ni—C_{aryl} bond originally existing in **3** has been cleaved. By and large, the spectroscopic data for **4** compare very favorably with those obtained for the closely related μ_2,η^2-aroyl complex *trans*-$(Me_3P)_2BrNi$-$(C(O)C_6H_4$-*o*-$CH_2)NiBr(PMe_3)$, whose structure has been unambiguously established by X-ray methods.[3]

The transformation displayed in Scheme I represents a rather unusual example of reversibility of isocyanide insertion into a transition metal carbon bond. Regardless of the mechanism of this process (the reaction could proceed through an inter- or intramolecular pathway, and we have no evidence in favor of either of these possibilities), the overall conversion of **1** into **4** by reaction with $CNBu^t$, corresponds to a successive insertion–deinsertion of the isocyanide into the Ni–CH_2 bond, followed by reinsertion into the Ni–$C_{aromatic}$ bond. Isocyanides are more prone than CO to undergo insertion reactions,[4] but the corresponding transformations are usually irreversible.[4a] In fact, while there is ample evidence about the reversibility of the latter process for carbon monoxide, there is very little information regarding the deinsertion of isocyanides.[5c,f] It appears reasonable to assume that the presence in **1** of two Ni–C bonds of dissimilar nature, and hence with distinct kinetic and thermodynamic preferences, makes possible the observation of the above transformation.

The discerned thermodynamic preference for the CNR insertion into the Ni–C bonds of **1**, viz. Ni–Ar > Ni–η^3-CH_2Ar, coincides with that previously demonstrated for the analogous **1**–CO system.[3] By similarity with the insertion of $CNBu^t$ and in view of the fact that in this kind of complex the insertion of CO is usually under thermodynamic control, it seems likely that the kinetic product of the CO insertion reaction is an undetected (even at −80 °C) η^2-acyl analogous to **3a**–**3b**. It also seems likely that a CNXy complex analogous to **4** may exist. Unfortunately, no reaction is observed when **2** is heated in acetone at 40 °C and at higher temperatures only decomposition products are obtained.

Amide Formation by Coupling of Acyl and Imidoyl Functionalities. The existence in compounds **2** and **3** of a Ni–C bond makes them susceptible to undergo further insertion chemistry. The simpler CNXy system, i.e. complex **2**, has been chosen for this study, and in view of the facility with which CO inserts into the Ni–C bonds of complexes of this type[7b,13,17] the corresponding transformation has been investigated. Interest in this reaction was further enhanced by the possibility of generating a molecule containing an acyl and an imidoyl functionality on adjacent metal centers.

In a not completely clean process, complex **2** reacts with an excess of CO (20 °C, 1 atm) in the manner depicted in Scheme II. Thus, the reaction does not stop at the acyl stage but instead a mononuclear vinyl complex of nickel, **5**, is obtained. Ni(0)–carbonyl species and HBr are also produced, the latter can be trapped in the form of $HNEt_3Br$ when the reaction is effected in the presence of NEt_3.

Scheme II

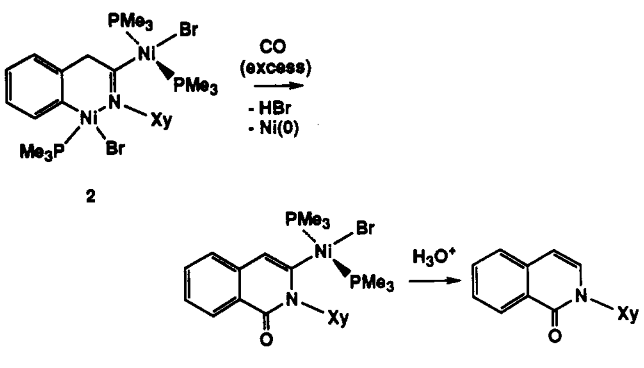

2

5

6

The two olefin carbons of **5** can be conclusively identified in the $^{13}C\{^1H\}$ NMR spectrum. One of them is a quaternary carbon directly bonded to the nickel atom in a *cis* position with respect to the two phosphine ligands (δ 155, t, $^2J_{CP}$ = 37 Hz), while the other undeniably exhibits ethylene character (δ 115, $^1J_{CH}$ = 163 Hz). The structure suggested for **5** is further confirmed by the generation of the *N*-aryl-1-isoquinolone **6** (Scheme II) by hydrolytic rupture of the Ni–C bond.

The amide functionality of **5** derives formally from the coupling of the imidoyl linkage of **2** with a molecule of CO. Although a mechanistic investigation has not been attempted, it seems feasible that CO inserts into the Ni–C bond of **2** to give an unstable seven-membered metallacycle which by extrusion of the Ni moiety and concurrent elimination of a proton from the methylene group would finally afford the observed product. The intramolecular coupling of aryl and imidoyl functionalities in high oxophilic early transition metal systems is known to occur with C–C bond formation.[4a,18] Our system, however, models an attested synthesis of cyclic amides by means of organometallic reagents.[19] Although the stoichiometric production of cyclic amides becomes therefore possible through the above set of reactions, the relatively low yield of the last step (i.e. the CO insertion, ca. 25%) and the amount of byproducts it generates severely limit the synthetic scope of this transformation.

Experimental Section

Microanalyses were by Pascher Microanalytical Laboratory, Remagen, Germany, and the Microanalytical Service of the University of Sevilla. Perkin-Elmer Models 577 and 684 spectrometers were used for the IR spectra, and a Varian XL-200 instrument was used for NMR studies. The ^{13}C NMR resonance of the solvent was used as an internal reference, but the chemical shifts are reported with respect to $SiMe_4$. ^{31}P NMR shifts are relative to external 85% H_3PO_4. All preparations and other operations were carried out under oxygen-free nitrogen using conventional Schlenk techniques. Solvents were dried and degassed before use. Complex **1**[3] and $CNBu^t$ [20] were prepared by published methods.

Synthesis of Complex 2. A cold (−60 °C) stirred solution of **1** (0.6 g, 1 mmol) in 40 mL of THF was treated with CNXy (0.13 g, 1 mmol) dissolved in 10 mL of THF. The cooling bath was

---

[16] For some recent examples of η^1-benzylic complexes of nickel, see: Carmona, E.; Marín, J. M.; Paneque, M.; Poveda, M. L. *Organometallics* **1987**, *6*, 1757. References 7b and 12c.

[17] Fryzuck, M. D.; McNeil, P. A.; Rettig, S. J. *J. Organomet. Chem.* **1987**, *332*, 345.

[18] Chamberlain, L. R.; Durfee, L. D.; Fanwick, P. E.; Kobriger, L. M.; Latesky, S. L.; McMullen, A. K.; Steffey, B. D.; Rothwell, I. P.; Folting, K.; Huffman, J. C. *J. Am. Chem. Soc.* **1987**, *109*, 6068.

[19] Colquhoun, H. M.; Holton, J.; Thompson, D. J.; Twigg, M. V. *New Pathways for Organic Synthesis*; Plenum Press: New York, 1984; Chapter 6.

[20] Gokel, G. W.; Widera, R. P.; Weber, W. P. *Org. Synth.* **1976**, *55*, 96.

removed and the solvent stripped off at room temperature. Extraction with 100 mL of Et_2O, filtration, concentration, and cooling at −30 °C furnished complex **2** as a crystalline material in 65% yield. ^1H NMR (200 MHz, CD_3COCD_3, 20 °C): δ 0.62 (d, 9 H, $^2J_{HP}$ = 9.5 Hz, PMe_3), 1.13 (d, 9H, $^2J_{HP}$ = 10.0 Hz, PMe_3), 1.81 (d, 9 H, $^2J_{HP}$ = 8.1 Hz, PMe_3), 2.54 (s, 3 H, C—Me), 3.21 (s, 1 H, C—Me), 5.02, 5.47 (d, d, 1 H, $^2J_{HH}$ = 16.0 Hz, CH_2), 7.18–8.30 (m, 7 H, aromatics). $^{31}P\{^1H\}$ NMR (81 MHz, CD_2Cl_2, 20 °C): δ −15.4 and −8.1 (AB spin system, $^2J_{AB}$ = 267 Hz, 2 *trans*-PMe_3), −7.0 (s, 1 PMe_3). $^{13}C\{^1H\}$ NMR (50 MHz, CD_2Cl_2): δ 14.9 (d, $^1J_{CP}$ = 29 Hz, PMe_3), 15.5 (d, $^1J_{CP}$ = 25 Hz, PMe_3), 15.7 (d, $^1J_{CP}$ = 31 Hz, PMe_3), 23.0 (d, J_{CP} = 10 Hz, C—*Me*), 24.2 (s, C—*Me*), 58.9 (d, J_{CP} = 12, $^1J_{CH}$ = 128 Hz, CH_2), 122.1, 123.5, 123.7, 125.0, 128.1, 129.0 (s, CH aromatics), 138.9 (d, J_{CP} = 10 Hz, CH aromatic), 123.8, 132.2, 136.7, 150.0 (s, quaternary aromatics), 153.6 (d, $^2J_{CP}$ = 44 Hz, Ni—C aromatic), 224.2 (t, $^2J_{CP}$ = 27 Hz, Ni—C=N–). IR (Nujol mull) ν(C=N) at 1495 (s) cm^{-1}. M_w (cryoscopically, C_6H_6, N_2) Calcd for **2**: 727. Found: 714. Anal. Calcd for **2**: C, 41.0; H, 5.7; N, 1.9. Found: C, 41.0; H, 5.9; N, 1.5.

Synthesis of Complex 3. To a cold (−80 °C) stirred solution of **1** (1.19 g, 2 mmol) in THF (100 mL) was slowly added a solution of $CNBu^t$ (0.23 mL, 2 mmol) in 20 mL of THF. The volatiles were removed *in vacuo* at 0 °C, and the residue was extracted with 100 mL of Et_2O. The resulting mixture was filtered and the filtrate cooled to −30 °C. Complex **3a** was obtained in this way as orange crystals which contained $^1/_4$ molecule of Et_2O per binuclear molecule of the complex. Yield: 65%.

Spectroscopic and analytical data for compound **3a**: $^{31}P\{^1H\}$ NMR (81 MHz, CD_2Cl_2, −70 °C) δ −15.1, −11.5 (AB spin system, $^2J_{AB}$ = 235 Hz, 2 *trans*-PMe_3), −9.5 (s, 1 PMe_3); $^{13}C\{^1H\}$ NMR (50 MHz, CD_2Cl_2, −45 °C) δ 14.3 (dd, $^1J_{CP}$ = 23, $^3J_{CP}$ = 6 Hz, PMe_3), 15.0 (d, $^1J_{CP}$ = 31 Hz, PMe_3), 15.5 (dd, $^1J_{CP}$ = 30, $^3J_{CP}$ = 7 Hz, PMe_3), 31.5 (s, C*Me*$_3$), 61.0 (s, CMe_3), 65.8 (s, $^1J_{CH}$ = 140 Hz, CH_2), 121.4, 122.5, 124.8 (s, CH aromatics), 137.6 (d, J_{CP} = 9 Hz, CH aromatic), 138.9 (s, quaternary aromatic), 154.5 (d, $^2J_{CP}$ = 22 Hz, Ni—C aromatic), 209.2 (t, $^2J_{CP}$ = 27 Hz, Ni—C=N–); IR (Nujol mull) ν(C=N) at 1530 (s) cm^{-1}. Anal. Calcd for **3**·$^1/_4$-Et_2O: C, 37.9; H, 6.5; N, 2.0. Found: C, 37.9; H, 6.4; N, 2.1.

Spectroscopic data for compound **3b**: ^1H NMR (200 MHz, CD_2Cl_2, 20 °C) δ 1.07 (pseudotriplet, 18 H, $J_{HP_{app}}$ = 3.8 Hz, 2 PMe_3), 1.14 (br, 9 H, 1 PMe_3), 1.43 (s, 9 H, CMe_3), 4.29 (s, 2 H, CH_2), 6.8–7.3 (m, 4 H, aromatics); $^{31}P\{^1H\}$ NMR (81 MHz, CD_2Cl_2, −70 °C) δ −9.2 (s, 2 PMe_3), −1.5 (s, 1 PMe_3); $^{13}C\{^1H\}$ NMR (50 MHz, CD_2Cl_2, 20 °C) δ 14.1 (pseudotriplet, $J_{CP_{app}}$ = 14 Hz, 2 PMe_3), 16.0 (d, $^1J_{CP}$ = 27 Hz, PMe_3), 29.5 (s, C*Me*$_3$), 36.8 (s, $^1J_{CH}$ = 129 Hz, CH_2), 59.2 (s, CMe_3), 122.1, 125.4, 126.6, 135.2 (s, CH aromatics), 139.0 (s, quaternary aromatic), 158.2 (t, $^2J_{CP}$ = 34 Hz, Ni—C aromatic), 169.2 (br s, Ni—C=N–); IR (CD_2Cl_2 solution) ν(C=N) at 1730 (s) cm^{-1}. M_w (cryoscopically, C_6H_6, N_2) Calcd for **3**: 572. Found: 592.

Synthesis of Compound 4. Complex **3a** (0.27 g, 0.4 mmol) was dissolved in 40 mL of acetone and the resulting solution was heated, with stirring, at 40 °C for 4 h. The solvent was evaporated under reduced pressure, and the residue was extracted with Et_2O. Filtration, concentration, and cooling at −30 °C afforded complex **4** as dark-red crystals in 55% yield. ^1H NMR (200 MHz, CD_2Cl_2, 20 °C): δ 1.03 (br d, 9 H, $^2J_{HP}$ = 6.8 Hz, PMe_3), 1.14 (d, 9 H, $^2J_{HP}$ = 9.2 Hz, PMe_3), 1.16 (br d, 2 H, $^3J_{HP}$ = 9.0 Hz, CH_2), 1.48 (br d, 9 H, $^2J_{HP}$ = 5.7 Hz, PMe_3), 2.46 (s, 9 H, CMe_3), 7.0–8.5 (m, 4 H, aromatics). $^{31}P\{^1H\}$ NMR (81 MHz, CD_2Cl_2): δ −21.2, −16.7 (AB spin system, $^2J_{AB}$ = 284 Hz, 2 *trans*-PMe_3), −13.8 (s, 1 PMe_3). $^{13}C\{^1H\}$ NMR (50 MHz, CD_2Cl_2): δ 13.5 (br d, $^1J_{CP}$ = 20 Hz, PMe_3), 14.9 (d, $^1J_{CP}$ = 29 Hz, PMe_3), 15.4 (br d, $^1J_{CP}$ = 20 Hz, PMe_3), 18.0 (d, $^2J_{CP}$ = 25, $^1J_{CH}$ = 140 Hz, CH_2), 32.7 (s, C*Me*$_3$), 63.0 (s, CMe_3), 123.1, 125.4, 130.3, 133.4 (s, CH aromatics), 138.2, 144.7 (s, quarternary aromatics), 204.4 (t, $^2J_{CP}$ = 27 Hz, Ni—C=N–). IR (Nujol mull): ν(C=N) at 1500 (s) cm^{-1}. Anal. Calcd for **4**: C, 37.1; H, 6.2; N, 2.1. Found: C, 36.9; H, 6.2; N, 1.7.

Table III. Crystal and Refinement Data for 2 and 3a

compd	2	3a
formula	$C_{25}H_{42}NP_3Br_2Ni_2$	$C_{21}H_{42}NP_3Br_2Ni_2$·$^1/_2C_4H_{10}O$
mol wt	726.8	715.8
cryst syst	monoclinic	monoclinic
space group	$P2_1/n$	$P2_1/n$
a, Å	12.437(3)	26.05(1)
b, Å	16.025(2)	10.226(1)
c, Å	16.015(2)	12.013(2)
β, deg	101.47(1)	93.54(2)
V, Å^3	3128.1(9)	3194(1)
Z	4	4
F(000)	1480	1468
ρ(calcd), g cm^{-3}	1.54	1.49
temp, °C	22	22
μ, cm^{-1}	39.1	38.26
cryst dimens, mm	0.2 × 0.4 × 0.3	0.2 × 0.2 × 0.3
scan technique	ω–2θ	ω–2θ
scan speed range, deg min^{-1}	1.5–16.48	1.26–16.48
θ	$1 < \theta < 25$	$1 < \theta < 25$
data collcd	(−17,0,0) to (17,22,22)	(−31,0,0) to (31,12,14)
no. of unique data	9113	5614
no. of unique data (I) ≥ 2σ(I)	3254	2324
decay	≤5%	≤60% variation
R(int), %	2.8	2.9
std rflns	3/84	3/58
$R = \sum\|\Delta F\|/\sum\|\Delta F_o\|$	5.2	7.4
weighing scheme	unit	unit
$R_w = (\sum w\Delta^2F/w\|F_o\|^2)^{1/2}$	5.7	8.2
max shift/error	0.5	0.6
abs corr range	0.93–1.10	0.92–1.18

Table IV. Fractional Coordinates for 2

atom	x/a	y/b	z/c	U_{eq},[a] Å^2
Ni1	0.05266(10)	0.14397(8)	0.77751(8)	340(4)
Ni2	0.35806(10)	0.28150(7)	0.72502(8)	336(4)
Br1	−0.11009(10)	0.12581(11)	0.83237(9)	784(6)
Br2	0.37897(10)	0.39048(7)	0.82802(7)	519(4)
P1	−0.04372(23)	0.14252(18)	0.64741(18)	463(9)
P2	0.14837(22)	0.09332(17)	0.90072(16)	402(9)
P3	0.53327(22)	0.25997(17)	0.74850(17)	424(9)
N	0.20286(58)	0.25791(45)	0.72798(47)	323(25)
C1	0.17651(72)	0.17977(56)	0.73822(53)	299(28)
C2	0.25720(77)	0.11409(54)	0.71889(61)	369(32)
C3	0.29957(78)	0.13257(60)	0.63911(61)	389(33)
C4	0.29361(96)	0.07316(70)	0.57564(72)	540(43)
C5	0.32507(102)	0.09428(82)	0.50014(78)	641(49)
C6	0.36179(95)	0.17348(78)	0.48645(64)	558(44)
C7	0.37298(82)	0.23110(67)	0.55376(66)	474(38)
C8	0.34531(76)	0.21031(62)	0.63094(59)	368(32)
C9	0.12583(75)	0.32532(59)	0.73167(68)	397(35)
C10	0.08865(85)	0.37086(64)	0.65486(71)	490(39)
C11	0.01388(100)	0.43461(69)	0.65486(87)	621(48)
C12	−0.02191(109)	0.45527(75)	0.72891(114)	777(62)
C13	0.01621(104)	0.41387(76)	0.80227(94)	681(53)
C14	0.09282(93)	0.34983(68)	0.80519(80)	557(44)
C15	0.13789(115)	0.31273(74)	0.89047(78)	652(52)
C16	0.12705(106)	0.35085(74)	0.57490(70)	610(46)
C17	0.02528(105)	0.13000(96)	0.56052(70)	762(55)
C18	−0.13677(100)	0.05387(75)	0.62852(82)	655(48)
C19	−0.13478(100)	0.23100(79)	0.61995(90)	741(54)
C20	0.11911(132)	−0.01796(73)	0.89881(83)	780(60)
C21	0.29723(91)	0.09833(86)	0.92957(72)	649(47)
C22	0.11204(103)	0.12417(79)	1.00006(66)	617(47)
C23	0.57394(105)	0.21913(100)	0.85551(76)	829(58)
C24	0.58896(95)	0.18130(79)	0.68869(88)	706(52)
C25	0.62605(99)	0.34733(74)	0.74378(90)	715(53)

[a] $U_{eq} = (1/3)\sum(U_{ij}a_i^*\cdot a_j^*\cdot \mathbf{a}_i\cdot \mathbf{a}_j \cos(\mathbf{a}_i,\mathbf{a}_j)) \times 10^4$.

Reaction of Complex 2 with CO. Through a solution of complex **2** (0.73 g, 1 mmol) in 40 mL of acetone was bubbled carbon monoxide at room temperature for 5 min. After evaporation of the volatiles under reduced pressure, the residue was extracted with Et_2O–CH_2Cl_2. Filtration, concentration, and cooling to −80 °C afforded complex **5** in several crops. Yield:

25%. ^{1}H NMR (200 MHz, CD_2Cl_2, 20 °C): δ 1.27 (pseudotriplet, 18 H, $J_{HP_{app}}$ = 3.9 Hz, 2 PMe_3), 2.10 (s, 6 H, 2 CMe), 6.20 (t, 1 H, $^4J_{HP}$ = 1.9 Hz, H—C=C—Ni), 7.3–8.2 (m, 7 H, aromatics). $^{31}P\{^1H\}$ NMR (81 MHz, CD_2Cl_2): δ −15.6 (s). $^{13}C\{^1H\}$ NMR (50 MHz, CD_2Cl_2): δ 14.7 (pseudotriplet, $J_{CP_{app}}$ = 15 Hz, 2 PMe_3), 19.2 (s, 2 C*Me*), 115.4 (t, $^3J_{CP}$ = 7 Hz, $^1J_{CH}$ = 163 Hz, Ni—C=*C*—H), 122.8, 123.8, 127.8, 128.3, 128.8, 132.2 (s, 1:1:1: 1:2:1 ratio, CH aromatics) 122.6, 136.1, 137.1, 141.3, (s, the second one of more intensity, quaternary aromatics), 155.3 (t, $^2J_{CP}$ = 37 Hz, Ni—*C*—CH), 163.1 (s, C=O). IR (nujol mull): ν(C=O) at 1620 (s), ν(C=C) at 1530 (s) cm^{-1}. Anal. Calcd for **5**: C, 51.2; H, 5.9; N, 2.6. Found: C, 50.9; H, 6.1; N, 2.3.

***N*-(2,6-dimethylphenyl)-1-isoquinolone, 6.** To a suspension of complex **5** (0.20 g, 0.4 mmol) in 30 mL of diethyl ether was added dichloromethane until complete dissolution. The resulting solution was stirred with 10 mL of 6 M H_2SO_4 for several hours. The organic phase was decanted and the aqueous layer washed with 20 mL of Et_2O. The combined organic extracts were dried over Na_2SO_4 and evaporated to dryness, and the residue was taken up in petroleum ether. Filtration and cooling at −30 °C furnished **6** as white crystals in almost quantitative yield. ^{1}H NMR (200 MHz, $CDCl_3$, 20 °C): δ 2.10 (s, 6 H, 2 CMe), 6.60, 6.90 (d, d, 1 H, 1 H, $^3J_{HH}$ = 7.4 Hz, HC=CH), 7.2–8.5 (m, 7 H, aromatics). $^{13}C\{^1H\}$ NMR (50 MHz, $CDCl_3$): δ 17.7 (2 C*Me*), 106.6, 125.9, 126.9, 128.2, 128.3, 128.5, 128.6, 131.6 (1:1:1:1:1:2:1:1 ratio, CH aromatics and olefins), 125.8, 132.4, 137.2, 139.4 (the second one of more intensity, quaternary aromatics), 161.2 (C=O). IR (Nujol mull): 1630 (s), 1610 (m), 1570 (m), 1530 (s) cm^{-1}. MS: *m/e* 249. Anal. Calcd for **6**: C, 81.9; H, 6.0; N, 5.6. Found: C, 81.3; H, 6.1; N, 5.4.

X-ray Structure Determination. A summary of the fundamental crystal data is given in Table III. Prismatic crystals of **2** and **3a** were coated with an epoxy resin and mounted in a κ diffractometer with graphite monochromatized Mo Kα radiation (λ = 0.710 17 Å). The cell dimensions were refined by least-squares fitting the θ values of the 25 reflections with a 2θ range of 12–40° for **2** and 12–32° for **3a**. Due to the instability of **3a** a time limit of 45 s was adopted for the final scan of each reflection. The intensities were corrected for Lorentz and polarization effects. Scattering factors for neutral atoms and anomalous dispersion corrections for Ni, Br, and P were taken from ref 21. The structures were solved by Patterson and Fourier methods. An empirical absorption correction[22] was applied to the end of the isotropic refinement. For compound **3a**, some nonresolvable disorder from the thermal motion was found around the Et_2O molecule of crystallization, and the atoms involved in this group were refined isotropically.

Table V. Fractional Coordinates for 3a

atom	x/a	y/b	z/c	U_{eq},[a] Å^2
Ni1	−0.00004(9)	0.19443(22)	0.19254(19)	38(1)
Ni2	0.84870(9)	0.19564(24)	0.37803(19)	40(1)
Br1	0.52766(9)	0.08662(21)	0.73623(21)	69(1)
Br2	0.77070(8)	0.21194(28)	0.46780(20)	75(1)
P1	0.08021(19)	0.15248(50)	0.17138(44)	47(2)
P2	0.88083(20)	0.34723(50)	0.49490(44)	47(2)
P3	0.81808(19)	0.01205(51)	0.29647(45)	50(2)
N	0.92834(46)	0.23174(116)	0.22253(101)	26(5)
O	0.27340(341)	0.05710(911)	0.30170(718)	100(34)
C1	0.91092(64)	0.18463(168)	0.31194(158)	45(7)
C2	0.94991(70)	0.10245(170)	0.37946(150)	45(7)
C3	0.96766(60)	−0.01093(168)	0.31236(149)	37(6)
C4	0.98447(64)	0.01410(172)	0.20843(143)	38(6)
C5	0.99174(70)	−0.09651(191)	0.13835(163)	54(7)
C6	0.98334(69)	−0.22252(152)	0.17892(181)	49(7)
C7	0.97066(71)	−0.24385(188)	0.28407(164)	47(7)
C8	0.96139(74)	−0.13926(190)	0.35102(162)	50(7)
C9	0.89524(70)	0.31858(164)	0.14211(156)	49(7)
C10	0.89009(83)	0.45439(189)	0.19245(162)	61(8)
C11	0.84320(72)	0.25963(190)	0.11417(137)	51(7)
C12	0.92385(85)	0.32942(190)	0.03315(157)	62(8)
C13	0.23770(423)	−0.04750(1153)	0.29770(932)	92(20)
C14	0.25650(397)	−0.11630(1053)	0.22320(866)	81(20)
C15	0.26220(371)	0.21070(1055)	0.30040(814)	77(19)
C16	0.27470(420)	0.27410(1175)	0.38450(921)	97(20)

[a] $U_{eq} = (1/3)\,(U_{ij}a_i^{*}\cdot a_j^{*}\cdot \mathbf{a}_i\cdot \mathbf{a}_j \cos(\mathbf{a}_i,\mathbf{a}_j)) \times 10^3$.

A final refinement was undertaken with unit weight and fixed isotropic factors and coordinates for all H atoms, for both compounds. Due to damage of the crystal of **3a**, in the course of the data collection (see Table III), the spectrum was very poor, and because of this, it has not proved possible to get a good weighting scheme and better refinement for this compound. Most calculation was carried out with the X-ray 80 system.[23]

Acknowledgment. We thank the Spanish Ministry of Education (J.C.) for a research grant. We gratefully acknowledge generous financial support from the Dirección General de Investigación Científica y Técnica (Proyecto PB-87201) and Junta de Andalucía. Thanks are also due to the University of Sevilla for use of analytical and NMR facilities.

Supplementary Material Available: Tables of H atom coordinates and thermal parameters (4 pages). Ordering information is given on any current masthead page.

OM930196U

---

(21) *International Tables for X-Ray Crystallography*; Kynoch Press: Birmingham, U.K., 1974; Vol. IV, p 72.

(22) Walker, N.; Stuart, D. *Acta Crystallogr.* **1983**, *A39*, 153.

(23) Stewart, J. M. *The X-Ray 80 System*; Computer Science Center, University of Maryland: Collegue Park, MD, 1985.